



Synthesis and biological evaluation of asymmetrical diarylpentanoids as antiinflammatory, anti- α -glucosidase, and antioxidant agents

Sze Wei Leong^{1,2} · Tahani Awin^{1,3} · Siti Munirah Mohd Faudzi^{1,4} · M. Maulidiani⁵ · Khozirah Shaari^{1,4} · Faridah Abas^{1,6}

Received: 29 May 2019 / Accepted: 17 August 2019 / Published online: 27 August 2019
© Springer Science+Business Media, LLC, part of Springer Nature 2019

Abstract

A series of seven new (**1**, **3**, **6**, **7**, **10**, **12**, and **13**) and six (**2**, **4**, **5**, **8**, **9**, and **11**) known diarylpentanoid analogs were synthesized and assessed for their nitric oxide (NO) and α -glucosidase inhibitory activities as well as their antioxidant capacity. Nine compounds (**2**, **3**, **4**, **5**, **6**, **8**, **11**, **12**, and **13**) were found to exhibit comparable activity to that of curcumin ($IC_{50} = 13.0 \mu M$), in which compound **8** has displayed strongest NO inhibitory activity with the IC_{50} values of $17.5 \mu M$. Meanwhile, four compounds (**1**, **7**, **12**, and **13**) were found to possess better α -glucosidase inhibitory activity than that of curcumin ($30.9 \mu M$), with the IC_{50} values ranging from 19.4 to $24.9 \mu M$. On the other hand, none of the synthesized compounds has achieved better DPPH scavenging activities than that of curcumin, indicating the relatively poor antioxidant potential of desired diarylpentanoid structure. Structure-activity relationship (SAR) study disclosed that the existence of *meta*-hydroxyphenyl and bromo groups is crucial for antiinflammatory and anti- α -glucosidase activities, respectively. Molecular docking study showed that bromo moiety could form additional hydrophobic contacts with α -glucosidase, thereby increased the inhibition of diarylpentanoid against α -glucosidase. The overall results suggested that diarylpentanoids with poly-*meta*-hydroxylated phenyl ring and multiple bromo groups may lead to the discovery of new diarylpentanoids with both antiinflammatory and anti- α -glucosidase activities.

Keywords Antiinflammatory · α -glucosidase · Antioxidant · Diarylpentanoids · Docking

Supplementary information The online version of this article (<https://doi.org/10.1007/s00044-019-02430-5>) contains supplementary material, which is available to authorized users.

✉ Faridah Abas
faridah_abas@upm.edu.my

- 1 Laboratory of Natural Products, Institute of Bioscience, Universiti Putra Malaysia, 43400 Serdang, Selangor, Malaysia
- 2 Department of Microbiology, Faculty of Biotechnology and Biomolecular Sciences, Universiti Putra Malaysia, 43400 Serdang, Selangor, Malaysia
- 3 Department of Chemistry, Faculty of Science, University of Benghazi, Benghazi, Libya
- 4 Department of Chemistry, Faculty of Science, Universiti Putra Malaysia, 43400 Serdang, Selangor, Malaysia
- 5 School of Fundamental Science, Universiti Malaysia Terengganu, 21030 Kuala Nerus, Terengganu, Malaysia
- 6 Department of Food Science, Faculty of Food Science and Technology, Universiti Putra Malaysia, 43400 Serdang, Selangor, Malaysia

Introduction

Curcumin is an important chemical constituent, which found mostly in the *Zingiberaceae* family with specific emphasis on *Curcuma* species (Akram et al. 2010). Being an excellent free radical scavenger and superoxide inhibitor, curcumin has attracted the interest of numerous researchers for its wide range of biological activities including but not limited to antiinflammatory, anticancer, and antioxidant (Bisht et al. 2010, Wu et al. 2010, Ben et al. 2011, Naik et al. 2011, Gupta et al. 2013). In addition, curcumin has been reported to be a respectable antimalarial and antibacterial agent due to its cytotoxic effect on numerous parasites and bacteria, such as *Plasmodium falciparum* and *Helicobacter pylori* (Cui et al. 2007, De et al. 2009). However, several reports revealed that curcumin is poor in stability and absorbability in body's circulating fluids, which resulting in low bioavailability, thus reducing its usefulness in clinical trials (Ravindranath and

Chandrasekhara 1981, Shoba et al. 1998, Pan et al. 1999). Therefore, several laboratories have entered intensive studies of synthetic modifications of curcumin in order to overcome the aforementioned challenges. The synthetic modification of curcumin has led to the discovery of diarylpentanoids, a 5-carbon spacer series of molecules with curcumin-like medicinal properties and enhanced stability (Lee et al. 2009, Ahmad et al. 2014).

Diarylpentanoids have been reported to display notable antiinflammatory potential due to their positive inhibitions on a diverse range of enzymes, pro-inflammatory cytokines, and mediators such as prostaglandins, nitric oxide (NO), and tumor necrosis factor alpha (Liang et al. 2008, Zhao et al. 2010, Fang et al. 2013). On top of these, diarylpentanoids were found to be more chemically and metabolically stable in both physiological pH and rat liver microsomes, making them a potent scaffold that worth to be developed as stable bioactive molecules (Zhang et al. 2014, Leong et al. 2015).

NO is a short lived free radical molecule, which synthesized endogenously from arginine, molecular oxygen, and NADPH during a complex reaction catalyzed by several nitric oxide synthases (NOS). Although NO is released as one of the primary defensive mechanisms in human's body in response to pathogen invasion, the overproduction of such molecules may promote tissue injuries through cell lipids peroxidation and deoxyribonucleic acid mutation, which in turn lead to diverse diseases including arthritis, cardiovascular disorders, ulcerative colitis, and cancer (Rachmilewitz et al. 1995, Sharma et al. 2007, Choudhari et al. 2013). Therefore, suppressing NO production may be an efficient strategy in the search of multi-functional drugs. Interestingly, previous study showed that the inhibition of NOS could reduce the glucose uptake in diabetes patients, which suggests that dual inhibition of NO and α -glucosidase, a key enzyme of glucose metabolism, could be an alternative strategy in treating diabetes (Kingwell et al. 2002). Based upon these, the aim of this study is to synthesize a series of stable 2,6-dibenzylidenecyclohexanone analogs and evaluate for their antiinflammatory, anti- α -glucosidase, and antioxidant activities.

Materials and methods

Chemistry

All chemicals and reagents were obtained from Sigma-Aldrich (St. Louis, MO, USA) and Merck (Darmstadt, Germany) companies. Solvents were purchased from common commercial suppliers, were dried and distilled before use. To observe the reaction progress, thin-layer chromatography was

regularly performed on TLC plate (0.20 mm Merck silica gel 60 F254) in each reaction stage. Purification processes were performed by using column chromatography on silica gel 60 (mesh 70–230, Merck). Mass spectra were measured using a gas chromatography-mass spectrometer GCMS-QP2010 Ultra (Shimadzu, Kyoto, Japan) Mass Spectrometer. Nuclear Magnetic Resonance spectra were recorded using a Varian 500 MHz NMR Spectrometer (Varian Inc., Palo Alto, CA).

General procedure for the synthesis of diarylpentanoid analogs

Catalytic amount of *p*-toluenesulphonic acid was added into the 30 mL toluene that contains a mixture of 20 mmol each of cyclohexanone and pyrrolidine. The solution was kept in 100 mL SNRB flask at room temperature with subsequent refluxed on a Dean & Stark apparatus for 2 h in order to produce (I). Upon completion, 20 mL of toluene containing 20 mmol of 4-hydroxybenzaldehyde or 3-hydroxybenzaldehyde was added dropwise into the reaction mixture and stirred for 24 h. Subsequently, 10 mL of deionised water was added into the solution and refluxed for 30 min. The resulting solution was extracted thrice with 3 M HCl and once with water. The toluene layer obtained was then dried over anhydrous MgSO₄ and concentrated in vacuo to yield the crudes of II and III. After purification with column chromatography, II and III were dissolved in 20 mL of acetic acid followed by the addition of appropriate benzaldehydes and catalytic amount of sulfuric acid. The resulting reaction mixtures were stirred at room temperature overnight. Upon completion, the reaction mixtures were added with 100 mL of distilled water and stirred for 5 min, followed by three times extractions with 100 mL of ethyl acetate. The organic layer obtained was then washed with saturated sodium bicarbonate solution (NaHCO₃) and dried over anhydrous MgSO₄ to obtain the crude of targeted compounds (IV). The crude products were then purified on column chromatography (Leong et al. 2018a, 2018b).

2-(4-Hydroxybenzylidene)-6-(3-bromobenzylidene)cyclohexanone (1)

Yellow amorphous powder (19.02%), m. p. 83–85 °C. ¹H-NMR (500 MHz, C₃D₆O, δ ppm): 8.83 (s, 1H), 7.68 (s, 1H), 7.67 (s, 1H), 7.61 (s, 1H), 7.56 (d, *J* = 8 Hz, 1H), 7.52 (d, *J* = 8 Hz, 1H), 7.48 (d, *J* = 8.5 Hz, 2H), 7.43 (d, *J* = 8 Hz, 1H), 6.95 (d, *J* = 8.5 Hz, 2H), 2.97–2.92 (m, 4H), 1.83–1.79 (m, 2H). ¹³C-NMR (125 MHz, C₃D₆O, δ ppm): 191.2, 158.4, 139.8, 139.2, 136.8, 136.0, 132.4, 131.9, 131.3, 130.2, 129.5, 128.2, 127.3, 121.3, 115.4, 28.1, 28.0, 22.7. EIMS, *m/z*: 369.30 (M⁺).

2,6-Bis(4-hydroxybenzylidene)cyclohexanone (2)

Yellow amorphous powder (53.72%), m. p. 209–210 °C. ¹H-NMR (500 MHz, C₃D₆O, δ ppm): 8.71 (s, 2H), 7.64 (s, 2H), 7.45 (d, *J* = 8.5 Hz, 4H), 6.93 (d, *J* = 8.5 Hz, 4H), 2.95–2.92 (m, 4H), 1.82–1.77 (m, 2H). ¹³C-NMR (125 MHz, C₃D₆O, δ ppm): 188.5, 158.1, 135.8, 133.7, 132.4, 129.4, 115.5, 28.3, 22.9. EIMS, *m/z*: 306.11 (M⁺).

2-(4-Hydroxybenzylidene)-6-(3-methoxybenzylidene)cyclohexanone (3)

Yellow amorphous powder (26.31%), m. p. 119–121 °C. ¹H-NMR (500 MHz, C₃D₆O, δ ppm): 8.81 (s, 1H), 7.66 (t, *J* = 5 Hz, 2H), 7.47 (d, *J* = 8.5 Hz, 2H), 7.38 (t, *J* = 7.4 Hz, 1H), 7.10 (d, *J* = 8 Hz, 1H), 7.06 (s, 1H), 6.96 (d, *J* = 2.5 Hz, 1H), 6.94 (d, *J* = 9 Hz, 2H), 3.85 (s, 3H), 2.96–2.93 (m, 4H), 1.82–1.77 (m, 2H). ¹³C-NMR (125 MHz, C₃D₆O, δ ppm): 191.7, 159.2, 158.3, 138.8, 137.9, 135.3, 135.1, 132.5, 132.3, 129.4, 128.5, 122.0, 115.4, 114.6, 113.3, 54.6, 28.3, 28.2, 22.8. EIMS, *m/z*: 320.05 (M⁺).

2-(4-Hydroxybenzylidene)-6-(3,4-dimethoxybenzylidene)cyclohexanone (4)

Yellow amorphous powder (17.80%), m. p. 180–182 °C. ¹H-NMR (500 MHz, C₃D₆O, δ ppm): 8.76 (s, 1H), 7.65 (d, *J* = 2 Hz, 2H), 7.46 (d, *J* = 8.5 Hz, 2H), 7.14 (dd, *J* = 8.5, 3.5 Hz, 2H), 7.04 (d, *J* = 8.5 Hz, 1H), 6.93 (d, *J* = 8.5 Hz, 2H), 3.87 (s, 3H), 3.86 (s, 3H), 2.99–2.93 (m, 4H), 1.82–1.77 (m, 2H). ¹³C-NMR (125 MHz, C₃D₆O, δ ppm): 186.4, 157.3, 149.7, 149.5, 137.3, 136.2, 135.5, 135.2, 132.5, 129.5, 128.5, 121.6, 115.4, 111.5, 110.7, 55.9, 28.4, 28.2, 22.9. EIMS, *m/z*: 350.05 (M⁺).

2-(4-Hydroxybenzylidene)-6-(3,4,5-trimethoxybenzylidene)cyclohexanone (5)

Yellow amorphous powder (11.29%), m. p. 78–79 °C. ¹H-NMR (500 MHz, C₃D₆O, δ ppm): 8.79 (s, 1H), 7.65 (s, 1H), 7.62 (s, 1H), 7.46 (d, *J* = 8.5 Hz, 2H), 6.94 (d, *J* = 9 Hz, 2H), 6.84 (s, 2H), 3.89 (s, 6H), 3.77 (s, 3H), 3.01–2.93 (m, 4H), 1.82–1.78 (m, 2H). ¹³C-NMR (126 MHz, C₃D₆O, δ ppm): 191.0, 158.4, 153.1, 139.7, 139.3, 136.8, 136.0, 135.9, 132.5, 130.2, 128.3, 115.5, 111.3, 58.9, 55.5, 28.3, 28.0, 22.8. EIMS, *m/z*: 380.15 (M⁺).

2-(4-Hydroxybenzylidene)-6-(3-hydroxybenzylidene)cyclohexanone (6)

Yellow amorphous powder (19.00%), m. p. 200–202 °C. ¹H-NMR (500 MHz, C₃D₆O, δ ppm): 8.80 (s, 1H), 8.49 (s, 1H), 7.65 (s, 1H), 7.61 (s, 1H), 7.46 (d, *J* = 5 Hz, 2H), 7.32

(t, *J* = 8 Hz, 1H), 7.00 (d, *J* = 5 Hz, 2H), 6.94 (d, *J* = 9 Hz, 2H), 6.87 (dd, *J* = 8.5, 2 Hz, 2H), 2.96–2.92 (m, 4H), 1.82–1.77 (m, 2H). ¹³C-NMR (125 MHz, C₃D₆O, δ ppm): 188.4, 158.2, 157.3, 137.4, 136.6, 136.3, 135.3, 133.7, 132.4, 129.5, 127.4, 121.7, 116.7, 115.6, 115.5, 28.4, 28.3, 22.8. EIMS, *m/z*: 306.12 (M⁺).

2-(4-Hydroxybenzylidene)-6-(4-bromobenzylidene)cyclohexanone (7)

Yellow amorphous powder (20.51%), m. p. 230–231 °C. ¹H-NMR (500 MHz, C₃D₆O, δ ppm): 8.80 (s, 1H), 7.66–7.62 (m, 4H), 7.49–7.45 (t, *J* = 9 Hz, 4H), 6.94 (d, *J* = 9 Hz, 2H), 2.97–2.91 (m, 4H), 1.82–1.78 (m, 2H). ¹³C-NMR (125 MHz, C₃D₆O, δ ppm): 191.0, 158.4, 136.0, 133.7, 132.4, 131.2, 130.2, 129.5, 128.2, 121.3, 115.5, 27.6, 20.9. EIMS, *m/z*: 369.05 (M⁺).

2,6-Bis(3-hydroxybenzylidene)cyclohexanone (8)

Yellow amorphous powder (32.24%), m. p. 205–206 °C. ¹H-NMR (500 MHz, C₃D₆O, δ ppm): 8.50 (s, 2H), 7.62 (s, 2H), 7.31 (t, *J* = 8 Hz, 2H), 7.01 (d, *J* = 7 Hz, 4H), 6.88 (dd, *J* = 9.5, 2.5 Hz, 2H), 2.96–2.93 (m, 4H), 1.82–1.77 (m, 2H). ¹³C-NMR (125 MHz, C₃D₆O, δ ppm): 192.1, 157.4, 135.6, 134.5, 129.4, 128.6, 121.0, 115.6, 114.9, 28.2, 22.7. EIMS, *m/z*: 306.00 (M⁺).

2-(3-Hydroxybenzylidene)-6-(3-methoxybenzylidene)cyclohexanone (9)

Yellow amorphous powder (20.63%), m. p. 147–148 °C. ¹H-NMR (500 MHz, C₃D₆O, δ ppm): 8.51 (s, 1H), 7.66 (s, 1H), 7.63 (s, 1H), 7.38 (t, *J* = 8 Hz, 1H), 7.30 (t, *J* = 8 Hz, 1H), 7.11 (d, *J* = 8 Hz, 1H), 7.07 (s, 1H), 7.02 (d, *J* = 8.5 Hz, 2H), 6.97 (dd, *J* = 8.5, 2.5 Hz, 1H), 6.88 (dd, *J* = 9, 1.5 Hz, 1H), 3.85 (s, 3H), 2.98–2.94 (m, 4H), 1.82–1.80 (m, 2H). ¹³C-NMR (125 MHz, C₃D₆O, δ ppm): 192.1, 159.7, 156.8, 135.6, 135.4, 134.7, 134.4, 129.5, 129.4, 128.7, 128.6, 121.9, 120.9, 116.6, 116.0, 115.6, 115.3, 54.6, 28.4, 24.3, 22.7. EIMS, *m/z*: 320.20 (M⁺).

2-(3-Hydroxybenzylidene)-6-(4-methoxybenzylidene)cyclohexanone (10)

Yellow amorphous powder (23.75%), m. p. 145–146 °C. ¹H-NMR (500 MHz, C₃D₆O, δ ppm): 8.51 (s, 1H), 7.67 (s, 1H), 7.62 (s, 1H), 7.54 (d, *J* = 8.5 Hz, 2H), 7.29 (t, *J* = 8 Hz, 1H), 7.03 (m, 4H), 6.87 (m, 1H), 3.86 (s, 3H), 2.97–2.92 (m, 4H), 1.82–1.77 (m, 2H). ¹³C-NMR (125 MHz, C₃D₆O, δ ppm): 191.7, 160.1, 156.9, 138.2, 136.5, 135.2, 134.7, 132.2, 131.7, 130.9, 128.6, 120.9, 116.1, 113.9, 113.0, 54.8, 28.2, 28.3, 22.8. EIMS, *m/z*: 320.10 (M⁺).

2-(3-Hydroxybenzylidene)-6-(3,4-dimethoxybenzylidene)cyclohexanone (11)

Yellow amorphous powder (15.67%), m. p. 163–165 °C. ¹H-NMR (500 MHz, C₃D₆O, δ ppm): 8.52 (s, 1H), 7.66 (s, 1H), 7.62 (s, 1H), 7.29 (t, *J* = 8.5 Hz, 1H), 7.16 (d, *J* = 6 Hz, 2H), 7.05 (d, *J* = 9 Hz, 1H), 7.00 (d, *J* = 7 Hz, 2H), 6.87 (dd, *J* = 7.5, 2 Hz, 1H), 3.89 (s, 3H), 3.87 (s, 3H), 3.00–2.93 (m, 4H), 1.83–1.78 (m, 2H). ¹³C-NMR (125 MHz, C₃D₆O, δ ppm): 191.7, 159.2, 149.8, 138.7, 137.9, 136.1, 135.3, 132.5, 131.3, 129.9, 128.6, 127.4, 115.4, 114.6, 114.2, 113.3, 54.6, 54.5, 28.4, 28.2, 22.8. EIMS, m/z: 350.10 (M⁺).

2-(3-Hydroxybenzylidene)-6-(3-bromobenzylidene)cyclohexanone (12)

Yellow amorphous powder (13.42%), m. p. 157–159 °C. ¹H-NMR (500 MHz, C₃D₆O, δ ppm): 8.53 (s, 1H), 7.69 (s, 1H), 7.63 (d, *J* = 5.5 Hz, 2H), 7.57 (d, *J* = 5.5 Hz, 1H), 7.54 (d, *J* = 7.5 Hz, 1H), 7.43 (t, *J* = 8 Hz, 1H), 7.30 (t, *J* = 8 Hz, 1H), 7.02 (dd, *J* = 7, 1 Hz, 2H), 6.88 (m, 1H), 2.97–2.93 (m, 4H), 1.82–1.79 (m, 2H). ¹³C-NMR (125 MHz, C₃D₆O, δ ppm): 191.5, 156.9, 136.0, 135.3, 134.0, 132.6, 132.5, 131.6, 131.1, 130.3, 129.5, 128.7, 128.2, 121.6, 120.9, 116.1, 115.0, 28.4, 28.3, 22.6. EIMS, m/z: 369.05 (M⁺).

2-(3-Hydroxybenzylidene)-6-(4-bromobenzylidene)cyclohexanone (13)

Yellow amorphous powder (12.63%), m. p. 192–193 °C. ¹H-NMR (500 MHz, C₃D₆O, δ ppm): 8.53 (s, 1H), 7.65 (s, 2H), 7.63 (d, *J* = 3.5 Hz, 2H), 7.50 (d, *J* = 8.5 Hz, 2H), 7.30 (t, *J* = 8 Hz, 1H), 7.01 (m, 2H), 6.88 (dd, *J* = 9.5, 2 Hz, 1H), 2.97–2.92 (m, 4H), 1.83–1.78 (m, 2H). ¹³C-NMR (125 MHz, C₃D₆O, δ ppm): 191.0, 158.5, 139.7, 139.3, 136.8, 135.6, 133.7, 133.3, 131.9, 131.7, 128.9, 127.3, 121.1, 115.5, 114.7, 28.3, 28.0, 22.8. EIMS, m/z: 369.05 (M⁺).

Cell culture

RAW 264.7 murine macrophage cells acquired from the American Type Culture Collection (Rockville, MD) were cultured as monolayer cultures in T75² cell culture flasks in Dulbecco's Modified Eagle's Medium (DMEM) with phenol red containing HEPES, L-glutamine supplemented with 10% fetal bovine serum, and 1% antibiotic solution (Gibco/BRL Life Technologies Inc, Eggenstein, Germany) under 5% CO₂ at 37 °C (Mohd Faudzi et al. 2015).

NO inhibition assay

The RAW 264.7 cells at 90–95% confluence were detached and seeded into a 96-well culture plate at a density of 5 × 10⁴ cells/well and allowed to attach for 24 h. Then, the cells were stimulated with 1 μg/mL of LPS (*Escherichia coli*, serotype 0111:B4) and 1 ng/mL of interferon-gamma (IFN-γ) in the presence or absence of the test compounds for 17 h. The nitrite production was then determined by Griess assay. Concisely, 50 μL of Griess reagent (1% sulfanilamide and 0.1% N-(1-naphthyl)-ethylenediamine dihydrochloride in 2.5% phosphoric acid) was added to 50 μL of cell culture supernatant for 15 min. The optical density was recorded at 550 nm using a microplate reader Spectramax Plus (Molecular Devices LLC, Sunnyvale, CA, USA) (Mohd Faudzi et al. 2015).

Cytotoxicity determination (MTT assay)

In each well, cell culture medium was replaced with 100 μL of 0.5 mg/ml MTT-containing DMEM followed by 4 h incubation at 37 °C in a 95% air and 5% CO₂ atmosphere. Upon completion, the supernatants in all wells were then removed, and the formazan salts formed were dissolved in 100% dimethyl sulfoxide (DMSO). After 15 min of incubation at room temperature, the absorbance was recorded at 570 nm using a microplate reader (Mohd Faudzi et al. 2015).

α-Glucosidase inhibitory activity assay

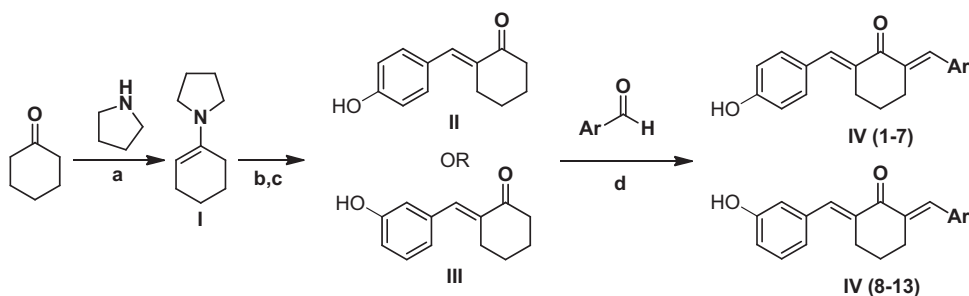
The α-glucosidase inhibitory assay was measured based on the previously reported method [27]. The samples were prepared by dissolving compounds **1–13** in DMSO-containing buffer. The substrate, *p*-nitrophenyl-α-D-glucopyranoside (PNPG) was prepared by dissolving it in 50 mM phosphate buffer (pH 6.5). For the assay, 96-well microplate that contains 10 μL of samples, 10 μL of enzyme, and 130 μL of buffer was incubated for 5 min at room temperature. Subsequently, 50 μL PNPG was added to each well and the plate was further incubated for 15 min at room temperature. Upon the completion, the reactions were stopped by adding 50 μL of 2 M glycine (pH 10) and left for 5 min in room temperature before the absorbance was recorded at 405 nm using SPECTRAMAX PLUS (Leong et al. 2018a, 2018b).

DPPH radical scavenging activity assay

In 96-well microplate, 100 μL of DPPH solution was added to 100 μL of different samples at different concentrations, of which both DPPH and samples were

Scheme 1 General synthetic steps for compounds **1–13**.

Chemical reagents and conditions: **a** *p*-toluene-sulfonic acid, toluene, reflux (2 h); **b** benzaldehyde, rt (24 h); **c** H₂O, reflux (0.5 h); **d** benzaldehyde, acetic acid, H₂SO₄, rt (overnight)



dissolved in 100% DMSO. The mixtures were then incubated in the dark for 30 min at a room temperature. Upon completion, the absorbance of each reaction mixture was measured at 517 nm using SPECTRAMax PLUS (Leong et al. 2016).

Molecular docking

Molecular docking studies were carried out using Discovery Studio 3.1 (Accelrys, San Diego, USA) on an Intel® (TM)2 Quad CPU Q8200 @2.33 GHz running under a Windows XP Professional environment. Since the crystal structure of *Saccharomyces cerevisiae* α -glucosidase is still not available, a homology model of α -glucosidase was built according to our previously reported method. The crystal structure of isomaltase (PDB: 3A4A) from *Saccharomyces cerevisiae* and α -glucosidase sequence (P53341) of *Saccharomyces cerevisiae* were obtained from the Protein Data Bank and UniProt (www.uniprot.org), respectively. Sequence alignment of P53341 on 3A4A was performed and homology models of α -glucosidase were built and validated using Modeler program. The model with the lowest modeler objective function was finally selected for ramachandran plot validation prior to molecular docking. Then, compound **7** and co-crystallized ligand (α -D-glucose) were drawn with ChemDraw Ultra 12.0 followed by ligands preparation protocol with the default setting recommended by Accelrys. The prepared ligands were then subjected to ligands minimization with CHARMm force field before being used for docking analyses. Minimized co-crystallized ligands were redocked into their respective enzymes with several sets of amino acids as flexible residues. The top ranked conformations resulted from the docking experiment were compared with their original crystallographic confirmation in terms of RMSD. The parameters with lowest RMSD values were selected for the flexible docking of compound **7** in the homology model. The flexible docking results were analyzed using Discovery Studio Visualizer v4.1.0.14169 (Accelrys, San Diego, USA) (Leong et al. 2018a, 2018b).

Results and discussion

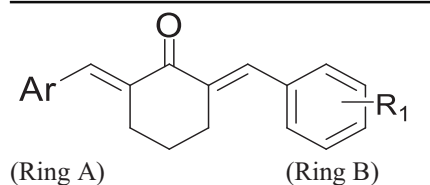
Chemistry

Compounds **1–13** (**IV**) were synthesized successfully via acidic aldol condensation as shown in Scheme 1. In detail, Intermediate **I** (N-(1-cyclohexenyl)pyrrolidine) was first achieved by reacting cyclohexanone and pyrrolidine on a Dean–Stark setup. In this step, Dean–Stark apparatus was used to remove the water side product formed during the enamine formation as water molecules could hydrolyse the desired intermediate **I** back to its precursors. Without any purification, the crude of intermediate **I** was directly reacted with 3- and 4-hydroxybenzaldehyde to form intermediates **II** and **III**, respectively. Upon purifications, **II** and **III** were further reacted with various benzaldehydes to produce the targeted compounds **IV** via acid-catalyzed aldol condensation reaction. The crudes of all compounds were purified using column chromatography and their chemical structures were confirmed through the ¹H-NMR, ¹³C-NMR (supplementary data) and mass spectrometry-based characterization.

NO inhibitory activity of diarylpentanoids

The synthesized 2,6-dibenzylidenecyclohexanone analogs (**1–13**) were assessed for their ability in inhibiting NO activity in IFN- γ /LPS-stimulated RAW 264.7 murine macrophage. The preliminary studies at 50 μ M testing concentration revealed that nine compounds (**2**, **3**, **4**, **5**, **6**, **8**, **11**, **12**, and **13**) have significantly suppressed the production of NO with the percentages of inhibition >50%. These nine bioactive compounds were further tested to determine their IC₅₀ values, and the values obtained were compared with that of curcumin as a positive control. MTT assay was subsequently performed to confirm that NO inhibition was not caused by the cytotoxicity of the synthesized analogs. The NO inhibition of synthesized 2,6-dibenzylidenecyclohexanones is shown in Table 1.

Among the tested analogs, compound **8** was found to exhibit the strongest NO inhibitory activity with the IC₅₀ value of 17.5 μ M. Meanwhile, the rest of eight compounds

Table 1 DPPH radical scavenging, NO, and α -glucosidase inhibitory activity of compounds 1–13


Compounds	Ar (ring A)	R ₁ (ring B)	NO inhibition (%) \pm SD	NO inhibition IC ₅₀ (μ M) \pm SD	Cytotoxicity IC ₅₀ (μ M) \pm SD	α -Glucosidase IC ₅₀ (μ M)	DPPH inhibition (%) 50 μ M	DPPH inhibition IC ₅₀ (μ M)
Curcumin	–	–	97.5 \pm 0.4	13.0 \pm 0.7	97.3 \pm 4.5	30.9 \pm 5.2	82.6 \pm 4.5	25.8 \pm 3.6
1	3-Bromophenyl	4'-OH	12.6 \pm 3.8	ND	ND	21.9 \pm 3.5	9.8 \pm 0.4	ND
2	4-Hydroxyphenyl	4'-OH	91.5 \pm 0.6	21.3 \pm 0.8	>100	34.9 \pm 4.6	31.1 \pm 1.2	ND
3	3-Methoxyphenyl	4'-OH	85.1 \pm 2.0	28.5 \pm 0.6	87.8 \pm 0.8	53.7 \pm 6.6	10.8 \pm 0.6	ND
4	3,4-Dimethoxyphenyl	4'-OH	74.3 \pm 1.2	26.1 \pm 0.5	>100	94.8 \pm 7.1	28.2 \pm 1.5	ND
5	3,4,5-Trimethoxyphenyl	4'-OH	80.5 \pm 4.2	22.8 \pm 1.1	>100	50.7 \pm 3.4	26.6 \pm 2.3	ND
6	3-Hydroxyphenyl	4'-OH	93.4 \pm 2.3	20.5 \pm 0.4	>100	25.0 \pm 0.5	31.2 \pm 0.8	ND
7	4-Bromophenyl	4'-OH	17.2 \pm 1.3	ND	ND	19.4 \pm 1.4	15.4 \pm 0.8	ND
8	3-Hydroxyphenyl	3'-OH	97.6 \pm 1.9	17.5 \pm 0.9	>100	35.2 \pm 1.7	19.7 \pm 0.4	ND
9	3-Methoxyphenyl	3'-OH	77.9 \pm 0.9	27.1 \pm 1.0	>100	50.3 \pm 2.2	10.6 \pm 0.7	ND
10	4-Methoxyphenyl	3'-OH	65.3 \pm 6.8	31.5 \pm 3.2	>100	59.1 \pm 2.5	12.5 \pm 1.4	ND
11	3,4-Dimethoxyphenyl	3'-OH	69.5 \pm 0.9	26.8 \pm 1.4	>100	95.2 \pm 6.7	11.5 \pm 0.5	ND
12	3-Bromophenyl	3'-OH	31.4 \pm 1.3	ND	ND	24.9 \pm 4.3	22.0 \pm 0.4	ND
13	4-Bromophenyl	3'-OH	25.7 \pm 2.6	ND	ND	23.8 \pm 2.1	14.7 \pm 1.9	ND

ND Not Determine

were found to display slightly weaker NO inhibitory activity as compared with that of compound **8**, with the IC₅₀ values ranging from 19.7 to 31.5 μ M. Structure-activity relationship (SAR) study revealed that hydroxyl group is crucial for antiinflammatory activity as all of the hydroxylated compounds (**6** and **8**) were found to possess better NO inhibitory activity than their respective methoxylated (**3** and **9**) and halogenated (**1** and **12**) analogs. On the other hand, comparison of *meta*- and *para*-substituted analogs revealed that *meta*-substitution is preferable as all of the *meta*-substituted diarylpentanoids (**8** and **9**) exhibit better NO inhibitory effects than their respective *para*-substituted analogs (**6** and **10**), regardless to the substituted functional groups. These results are in agreement with our previous studies, in which the *meta*-hydroxylated phenyl rings possess the strongest antiinflammatory activity. In addition to substitution pattern and substituted functional groups, electron density may also affect the NO inhibitory activity of synthesized compounds. This can be seen by comparing the NO inhibitory activity of all methoxylated compounds (**3**, **4**, **5**, **10**, and **11**), in which the multi-methoxylated diarylpentanoids (**4**, **5**, and **11**) showed improved NO inhibitory activity as compared with that of mono-methoxylated analogs (**3** and **10**). Since methoxy moiety is an electron donating functional group, this result is therefore implying that the higher the electron density of phenyl ring, the better the antiinflammatory activity of the compounds.

α -Glucosidase inhibitory activity of diarylpentanoids

Apart from antiinflammatory activity, all synthesized compounds were also tested for their α -glucosidase inhibitory activity. Based on the results obtained, four compounds (**1**, **7**, **12**, and **13**) were found to exhibit strong α -glucosidase inhibitory activities in which compound **7** has displayed the strongest activity with the IC₅₀ value of 19.4 μ M. Meanwhile, three other compounds (**2**, **6**, and **8**) have displayed moderate α -glucosidase inhibition, with the IC₅₀ values ranging from 25 to 35 μ M (Table 1). SAR study revealed that bromo group is important for α -glucosidase inhibitory activities as all of the brominated analogs (**1**, **7**, **12**, and **13**) are strong α -glucosidase inhibitors. Unlike NO inhibitory activity, the substitution position on the phenyl ring does not affect the anti- α -glucosidase potential of targeted compounds. This can be observed by comparing the *meta*-substituted compounds (**1**, **2**, and **12**) to their respective *para*-substituted analogs (**7**, **8**, and **13**) of which both *meta*- and *para*-substituted analogs possess similar activity.

In order to gain functional and structural insights into the binding mode of the most active analog (**7**) in α -glucosidase, molecular docking was performed with Discovery Studio 3.1. Since the crystal structure of *Saccharomyces cerevisiae* α -glucosidase is unavailable, a homology model of α -glucosidase was first built and validated using Discovery Studio 3.1 and Ramachandran plot, respectively,

Fig. 1 Binding interactions of compound 7 with the active site residues of α -glucosidase receptor

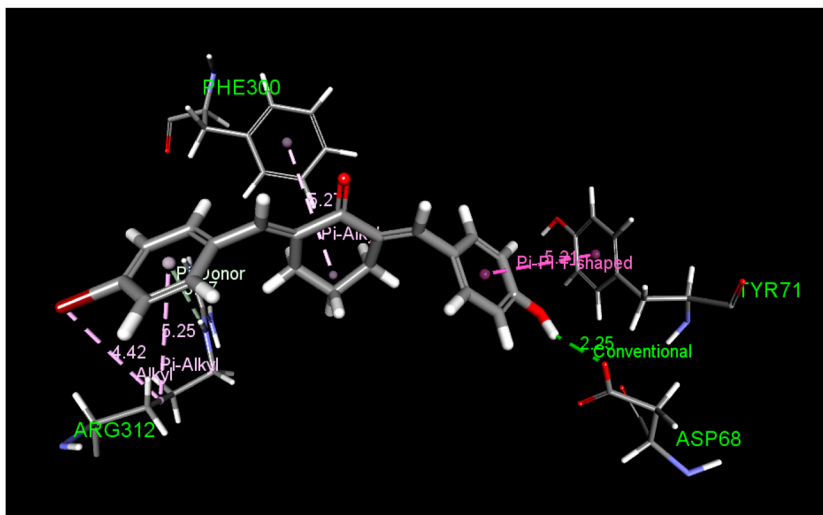


Table 2 Data resulted from the molecular docking of compounds 7 in α -glucosidase

Compound structure	Interacting amino acid residue	Bond type	Bonding distance (Å)
<p>Compound 7</p>	ASP68	Hydrogen bonding	2.25
	TRY71	Pi–Pi shaped	5.21
	PHE300	Pi–Alkyl	5.27
	ARG312	Pi–Alkyl	4.42
		Pi–Alkyl	5.25
		Pi–donar	3.17

followed by re-docking of co-crystallized ligands into the validated homology model. According to the result obtained (supplementary data), both homology model and flexible docking parameters were found to be acceptable as 100% of residues in homology built are located found in either favored (97.9%) or acceptable (2.1 %) regions while a RMSD value of 0.7147 Å was observed in the re-docking procedure. Figure 1 illustrated the binding interactions of compounds 7 in α -glucosidase.

As shown in Fig. 1, the hydroxyl and phenyl moieties of 4-hydroxyphenyl fragment of compound 7 interact with ASP68 and TYR71 residues through hydrogen bonding (green dashed line) and Pi–Pi shaped (purple dashed line) interactions, respectively. Meanwhile, the cyclohexanone fragment of the respective compound was found to interact with PHE 330 residue through Pi–Alkyl (light purple dashed line) hydrophobic interaction. Interestingly, both bromo and phenyl moieties of bromophenol fragment have displayed strong hydrophobic contacts including Pi–Alkyl (light purple dashed line) and Pi–donar (light green dashed line) interactions with ARG 312 residue. The multiple hydrophobic interactions of bromophenyl fragment thus explained the much better α -

glucosidase inhibitory effects of brominated compounds (1, 7, 12, and 13) as compared with the rest of the synthesized analogs. The molecular docking results of compounds 7 are summarized in Table 2.

DPPH scavenging activities of diarylpentanoids

Lastly, all synthesized compounds were evaluated for their antioxidant properties using 2,2-diphenyl-1-picrylhydrazyl (DPPH) scavenging assay. Noteworthy, none of the tested compounds showed significant DPPH scavenging activity at the testing concentration of 100 μ M. This indicates that mono- and di-hydroxylated diarylpentanoids are poor antioxidant. The result obtained are summarized in Table 1.

Conclusions

In summary, a series of seven new (1, 3, 6, 7, 10, 12, and 13) and six (2, 4, 5, 8, 9, and 11) diarylpentanoids were synthesized and evaluated for their anti-inflammatory, anti- α -glucosidase, and antioxidant activities. Compounds 7 and 8 were found to exhibit strongest anti- α -glucosidase and

antiinflammatory activity, respectively. SAR studies showed that *meta*-hydroxyphenyl is crucial for NO inhibitory activity, while bromo moiety is essential for enhanced anti- α -glucosidase activity. Subsequent molecular docking analysis revealed that additional hydrophobic interactions by bromo group is responsible for the enhanced anti- α -glucosidase activity of compound **7**. Since hydroxyl moiety is preferable to be substituted at the *meta*-position for NO inhibitory activity, while bromo moiety is independent to the substitution position for better α -glucosidase inhibition, we therefore concluded that 4-bromo-3-hydroxyphenyl-containing diarylpentanoid may be a new lead compounds with both antiinflammatory and anti- α -glucosidase properties.

Acknowledgements The authors thank the Ministry of Higher Education (MOHE) of Malaysia for financial support under the project FRGS/1/2014/ST01/UPM/02/1 (5538011).

Compliance with ethical standards

Conflict of interest The authors declare that they have no conflict of interest.

Publisher's note: Springer Nature remains neutral with regard to jurisdictional claims in published maps and institutional affiliations.

References

- Ahmad W, Kumolosasi E, Jantan I, Bukhari SN, Jasamai M (2014) Effects of novel diarylpentanoid analogues of curcumin on secretory phospholipase A2, cyclooxygenases, lipo-oxygenase, and microsomal prostaglandin E synthase-1. *Chem Biol Drug Des* 83:670
- Akram M, Shahab-ddin A, Ahmed K, Usmanhani A, Hannan E, Mohiuddin AM (2010) *Curcuma longa* and curcumin: a review article. *Rom J Biol -Plant Biol* 55:6
- Ben P, Liu J, Lu C, Xu Y, Xin Y, Fu J, Huang H, Zhang Z, Gao Y, Luo L, Yin Z (2011) Curcumin promotes degradation of inducible nitric oxide synthase and suppresses its enzyme activity in RAW 264.7 cells. *Int Immunopharmacol* 11:179
- Bisht K, Wagner KH, Bulmer AC (2010) Curcumin, resveratrol and flavonoids as anti-inflammatory, cyto- and DNA-protective dietary compounds. *Toxicology* 278:88
- Choudhari SK, Chaudhary M, Bagde S, Gadail AR, Joshi V (2013) Nitric oxide and cancer: a review. *World J Surg Oncol* 11:118
- Cui L, Miao J, Cui L (2007) Cytotoxic effect of curcumin on malaria parasite *Plasmodium falciparum*: inhibition of histone acetylation and generation of reactive oxygen species. *Antimicrob Agents Chemother* 51:488
- De R, Kundu P, Swarnakar S, Ramamurthy T, Chowdhury A, Nair GB, Mukhopadhyay AK (2009) Antimicrobial activity of curcumin against *Helicobacter pylori* isolates from India and during infections in mice. *Antimicrob Agents Chemother* 53:1592
- Fang X, Fang L, Gou S, Cheng L (2013) Design and synthesis of dimethylaminomethyl-substituted curcumin derivatives/analogues: potent antitumor and antioxidant activity, improved stability and aqueous solubility compared with curcumin. *Bioorg Med Chem Lett* 23:1297
- Gupta SC, Sung B, Kim JH, Prasad S, Li S, Aggarwal BB (2013) Multitargeting by turmeric, the golden spice: From kitchen to clinic. *Mol Nutr Food Res* 57:1510
- Kingwell BA, Formosa M, Muhlmann M, Bradley SJ, McConell GK (2002) Nitric oxide synthase inhibition reduces glucose uptake during exercise in individuals with type 2 diabetes more than in control subjects. *Diabetes* 51:2572
- Lee KH, Ab Aziz FH, Syahida A, Abas F, Shaari K, Israf DA, Lajis NH (2009) Synthesis and biological evaluation of curcumin-like diarylpentanoid analogues for anti-inflammatory, antioxidant and anti-tyrosinase activities. *Eur J Med Chem* 44:3195
- Leong SW, Abas F, Lam KW, Shaari K, Lajis NH (2016) 2-Benzoyl-6-benzylidenecyclohexanone analogs as potent dual inhibitors of acetylcholinesterase and butyrylcholinesterase. *Bioorg Med Chem* 24:3742
- Leong SW, Abas F, Lam KW, Yusoff K (2018a) In vitro and in silico evaluations of diarylpentanoid series as alpha-glucosidase inhibitor. *Bioorg Med Chem Lett* 28:302
- Leong SW, Chia SL, Abas F, Yusoff K (2018b) Asymmetrical meta-methoxylated diarylpentanoids: Rational design, synthesis and anti-cancer evaluation in-vitro. *Eur J Med Chem* 157:716
- Leong SW, Mohd Faudzi SM, Abas F, Mohd Aluwi MFF, Rullah K, Lam KW, Abdul Bahari MN, Ahmad S, Tham CL, Shaari K, Lajis NH (2015) Nitric oxide inhibitory activity and antioxidant evaluations of 2-benzoyl-6-benzylidenecyclohexanone analogs, a novel series of curcuminoid and diarylpentanoid derivatives. *Bioorg Med Chem Lett* 25:3330
- Liang G, Li X, Chen L, Yang S, Wu X, Studer E, Gurley E, Hylemon PB, Ye F, Li Y, Zhou H (2008) Synthesis and anti-inflammatory activities of mono-carbonyl analogues of curcumin. *Bioorg Med Chem Lett* 18:1525
- Mohd Faudzi SM, Leong SW, Abas F, Mohd Aluwi MFF, Rullah K, Lam KW, Abdul Bahari MN, Ahmad S, Tham CL, Shaari K, Lajis NH (2015) Synthesis, biological evaluation and QSAR studies of diarylpentanoid analogues as potential nitric oxide inhibitors. *MedChemComm* 6:1069
- Naik SR, Thakare VN, Patil SR (2011) Protective effect of curcumin on experimentally induced inflammation, hepatotoxicity and cardiotoxicity in rats: evidence of its antioxidant property. *Exp Toxicol Pathol* 63:419
- Pan MH, Huang TM, Lin JK (1999) Biotransformation of curcumin through reduction and glucuronidation in mice. *Drug Metab Dispos* 27:486
- Rachmilewitz D, Stamler JS, Bachwich D, Karmeli F, Ackerman Z, Podolsky DK (1995) Enhanced colonic nitric oxide generation and nitric oxide synthase activity in ulcerative colitis and Crohn's disease. *Gut* 36:718
- Ravindranath V, Chandrasekhara N (1981) Metabolism of curcumin—studies with [³H]curcumin. *Toxicology* 22:337
- Sharma JN, Al-Omran A, Parvathy SS (2007) Role of nitric oxide in inflammatory diseases. *Inflammopharmacology* 15:252
- Shoba G, Joy D, Joseph T, Majeed M, Rajendran R, Srinivas PS (1998) Influence of piperine on the pharmacokinetics of curcumin in animals and human volunteers. *Planta Med* 64:353
- Wu SH, Hang LW, Yang JS, Chen HY, Lin HY, Chiang JH, Lu CC, Yang JL, Lai TY, Ko YC, Chung JG (2010) Curcumin induces apoptosis in human non-small cell lung cancer NCI-H460 cells through ER stress and caspase cascade- and mitochondria-dependent pathways. *Anticancer Res* 30:2125
- Zhang Y, Zhao C, He W, Wang Z, Fang Q, Xiao B, Liu Z, Liang G, Yang S (2014) Discovery and evaluation of asymmetrical monocarbonyl analogs of curcumin as anti-inflammatory agents. *Drug Des Devel Ther* 8:373
- Zhao C, Cai Y, He X, Li J, Zhang L, Wu J, Zhao Y, Yang S, Li X, Li W, Liang G (2010) Synthesis and anti-inflammatory evaluation of novel mono-carbonyl analogues of curcumin in LPS-stimulated RAW 264.7 macrophages. *Eur J Med Chem* 45:5773